Multiphysics Simulation of a High Frequency Acoustic Microscope Lens

O. Tommiska[1], J. Mäkinen[1], A. Meriläinen[1], J. Hyvönen[1], A. Nolvi[1], T. Ylitalo[1], I. Kassamakov[1,2], A. Salmi[1*], E. Hæggström[1]

[1] Department of Physics, Division of Materials Physics, University of Helsinki, Helsinki, Finland
[2] Helsinki Institute of Physics, University of Helsinki, Helsinki, Finland
*Corresponding author (ari.salmi@helsinki.fi)

Abstract

High frequency ultrasound (100-1000 MHz) has been used in microscopy since the 1970s and the main imaging component, the acoustic transducer, is commercially available. With a broadband signal, the focus distance may vary across the frequency band. In this case, by knowing how the different frequencies focus, one can use this information to enhance the imaging resolution by taking into account the exact focus for the different frequency components.

We created a COMSOL Multiphysics® model of our scanning acoustic microscope's (SAM) transducer-lens system to study this effect. The simulation was done both in time- and in frequency domain. The resolution, working distance, and focal length depend on the lens structure, which is unique for each produced lens. To have the exact geometry of the outer surface of a commercial lens, we imaged one with a scanning white light interferometric (SWLI) 3D microscope and used the measured geometry in the simulations.

The presented results show the focus shape as a function of frequency. The results can be used in postprocessing to optimize the imaging resolution of our SAM.

Introduction

High frequency scanning acoustic microscopy (SAM) is a high resolution and non-destructive imaging technique that reveals both the surface and the subsurface structure, and properties of materials, such as elasticity [1] and porosity [2]. The image is created by performing a point scan across the area of interest and by analyzing the echoes reflected off the object [3]. When using a broadband signal, the transmitted signal contains many frequencies.

The SAM features of a piezo element, a lens, a coupling fluid, and an object that is imaged [4]. The lens is typically spherically concave and has an anti-reflection coating. The thickness of the anti-reflection coating is typically $\frac{1}{4}$ of the center wavelength [3].

Methods

The flat transducer in a SAM lens produces a plane wave pulse that refracts as it crosses the boundary of different media. The spherical concave shape of the lens surface focuses the acoustic waves, as they travel from the solid lens into the coupling fluid (Fig. 1).
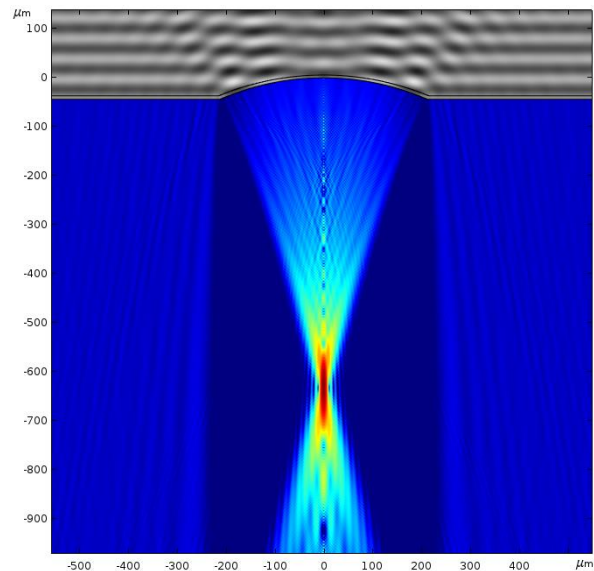

Figure 1: Schematic illustrating focusing of acoustic beams. The acoustic lens is visible on the top, and the focus point of acoustic beams in the middle (red colour).

1

The distance from the lens, at which the acoustic beams focus, when travelling from a solid to a liquid, can be solved analytically:

$$Z = R_c \left(\frac{sin(\theta_1)}{tan(\theta_1-\theta_2)} + 1 - cos(\theta_1) \right) \quad (1)$$

where Z is the focus distance, R_C is the curvature of the lens surface, θ_1 is the angle between the z-axis and surface normal at the point of refraction, and θ_2 is the angle between the surface normal and the wave beam in liquid [5].

With a small angle approximation ($\theta_1 << 1$) this becomes the 'lens makers equation'

$$Z_c = R_c \left(\frac{1}{1-\frac{C_2}{C_1}} \right) \quad (2)$$

where C_1 is the speed of sound in the lens and C_2 is the speed of sound in the coupling fluid [5].

Since Eq. 2 holds even for larger angles in the case of sapphire lenses [5], it is used to estimate the focal distance of our SAM [6].

Our SAM lens is made of sapphire and features a thin acoustic anti-reflection glass coating. Since the exact glass type is unknown, we used the parameters for soda-lime glass in the simulations. Since the designed center frequency of the lens was 250 MHz, the thickness of the anti-reflecting coating should be $\frac{1}{4}$ of wavelength of a 250 MHz wave in glass [3], $d_g \approx 5.8\mu m$. Values for material properties needed for the simulation were obtained from the literature (see Appendix Table 1).

To define the shape of the lens surface as accurately as possible, we imaged the lens with our scanning white light interferometric 3D microscope (SWLI) [7]. The SWLI data was analysed using MATLAB® R2018a software and an axisymmetric profile of the lens surface was created by collecting data points while rotating the 3D surface around its central axis (Fig. 2).
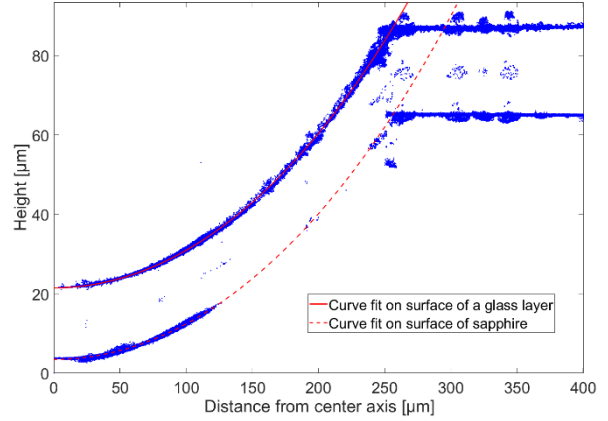

Figure 2: Surface profile and curves fitted to the circular part of the surface.

To analyze the lens curvature, the concave part of surface profile was selected by manually limiting the range of function fitting to only include the desired part. A spherical fit, Eq. 3, was made separately to each surface:

$$f_R(x) = -\sqrt{R_c^2 - x^2} + b \quad (3)$$

where R_C is the radius the circle, and b is the x-coordinate of the circle origin. From the fit, the radius of the glass layer surface was determined to be $R_{C1} = 533.25\pm0.15\mu m$ and the radius of surface of sapphire $R_{C2} = 563.38\pm0.33\mu m$. Using Eq. 2, the expected focal distance of our lens was $Z_0 \approx 621.88\mu m$.

This result does not consider effects caused by the anti-reflecting layer, since Eq. 2 only considers the case of refraction at the boundary between two different material domains. Despite this, the result can be used to judge the feasibility of the simulation results.

Since the SWLI measurements are done using light, the thickness of the anti-reflecting glass coating determined in Fig. 2 is the optical thickness. The actual thickness was solved from

$$d_g = \frac{OPL}{2n} \quad (4)$$

where OPL is the optical path length of light and n is the refractive index of the glass [8]. The thickness of the glass layer was solved to be $d_{g(centre)} = 5.84\mu m$ at the center of the lens and $d_{g(side)} = 7.07\mu m$ at the sides.

Simulation methods

The frequency-dependent focusing of our SAM was studied using the COMSOL Multiphysics® 5.3a simulation software. The simulation geometry comprised three material domains: sapphire, soda-lime glass, and water. Sapphire and soda-lime glass were introduced to the simulation as blank materials and their properties were set by hand. For water, a built-in "Water, liquid" material from the Material Library was used.

A Pressure Acoustics interface was used to study sound wave propagation in water, and a Solid Mechanics interface was used for the sapphire and glass. These two interfaces were coupled using the Acoustic-Structure interaction in Multiphysics. The simulation was done using 2D axisymmetric geometry, see Fig. 3.
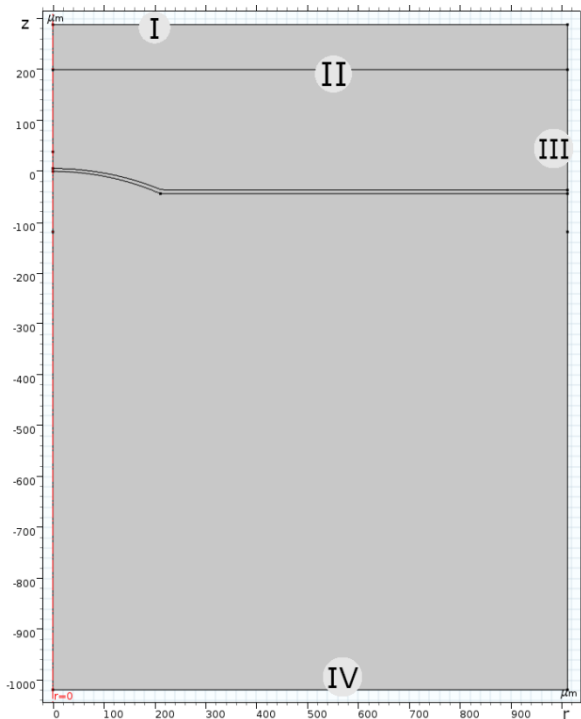

Figure 3: Geometry used in the frequency domain simulation. The two top parts are sapphire, the thin domain near $z = 0$ is soda-lime glass, and the large bottom part is water. Numbers in the picture mark boundaries with following boundary conditions: (I) Low-reflecting boundary, (II) Boundary load, (III) Roller, (IV) Plane wave radiation.

The mesh size was defined separately for each material domain. To determine the maximum size of the mesh element, the wavelength in each material was calculated and the maximum size was set to $\frac{1}{7}$ of that wave length.

In the simulations, the linear elastic material setting was used, both in the Pressure Acoustics and in the Solid Mechanics.

Acoustic waves were created using the "Boundary Load"-boundary condition. To prevent unwanted reflections from the top of the geometry as the simulation advances, the boundary load was placed inside the sapphire domain (II) and the top boundary of geometry (I) featured a low-reflecting boundary condition. Further, the boundary at -1000 µm (IV) had a "Plane Wave Radiation" boundary condition, whereas the right side of Solid Mechanics domain (III) featured the "Roller" boundary condition.

The simulations were first performed (due to computational efficiency) in the frequency domain, sweeping across 100 MHz-400 MHz with a step of 0.5 MHz. Subsequently, a time domain simulation was ran across the same frequency range, but with a larger 25 MHz step. In time domain, a five-cycle sine burst was used with a rectangular envelope.

Results from the time domain simulation were compared with the results of the frequency domain simulation to verify the frequency domain results.

Comparing the time- and frequency domain simulations showed much wave interference in the results of the frequency domain study. Interference was absent in the results of time domain study. This interference was large when the frequency was below 200 MHz. To confirm absence of interference in time domain, we performed a second time domain simulation, where we swept across 100 MHz-200 MHz, in 10 MHz steps. Since no interference was observed in these simulations, we decided to study whether the wave interference was caused by the geometric shape employed in the frequency domain simulation.

A convergence study was ran with different geometries in the frequency domain. The results of this study indicated that a wider geometry in frequency domain decreased the unwanted wave interference. Therefore, a wider geometry was selected for consecutive frequency domain simulations. Since no unwanted wave interference was observed in the time domain, the

original, narrower geometry was used for time domain simulation. The final geometry used in frequency domain simulations was 1000 µm wide whereas in the time domain simulation the geometry was 300 µm wide.

The simulation results were exported from COMSOL Multiphysics® using its export data functionality. For the analysis, two different kinds of data sets were exported: a 1D line along the $z = 0$ axis and a 2D grid, limited to the area around the expected focal point. For the frequency domain study, the square of the absolute acoustic pressure was evaluated. To have a comparable result from time domain study, the absolute acoustic pressure was evaluated and a square of the time integral of this data was calculated for each point of interest.

Results

To study the frequency dependence of the focal point distance, a Fourier series curve was fitted to the normalized 1D line data set for each frequency (one example is shown in Fig. 4). The fit was done to find the exact location of tallest peak. A Fourier series fit was used to approximate the behaviour of the acoustic intensity around the peak, since it is formed by constructive interference of waves [3].
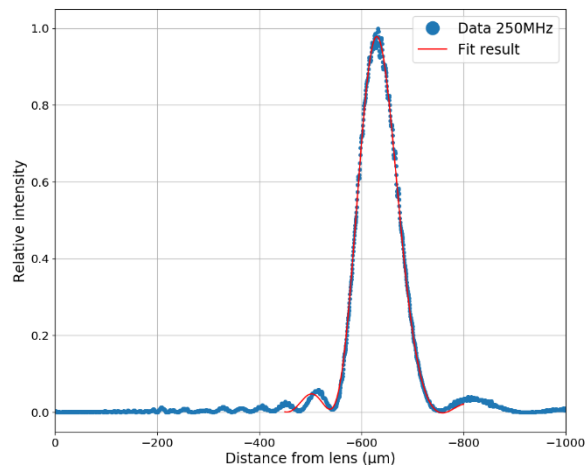

Figure 4: 1D line data (along z-axis) for 250 MHz excitation obtained in the frequency domain simulation. A Fourier series was fitted to the data and used in subsequent analysis.

The location of the peak at each frequency was determined by taking the maximum value of fitted curve and the results were plotted as a frequency-distance -plot, see Fig. 5.
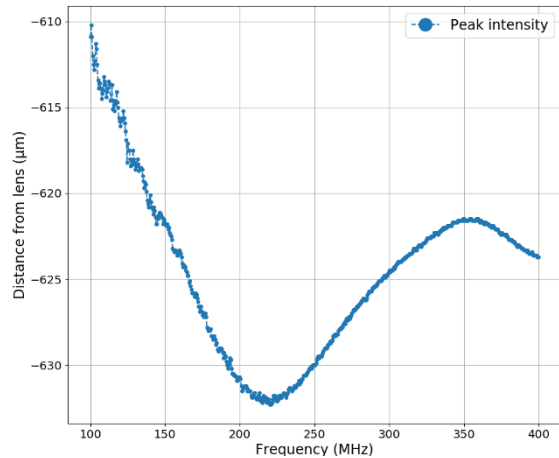

Figure 5: Distance to the intensity maximum as a function of frequency (frequency domain simulation).

To study the frequency dependence of the point of narrowest focus, the focal width was determined by a Gaussian fit (Fig. 6).
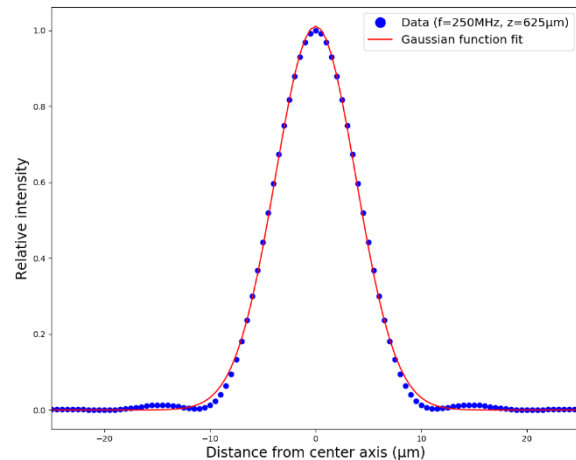

Figure 6: Gaussian curve fitted to frequency domain simulation data, taken along the r-axis, at $z=625\mu m$ and f=250 MHz.

The full width at half maximum (FWHM) values were then determined and plotted, Fig. 7. The frequency dependency of FWHM at focus is evident. Since the frequency dependence of FWHM showed an attenuating periodicity, an ansatz for the fit was made:

$$d_{focus} = a_0 + a_1 \sin\left(b_1 f^{b_2}\right) f^{-c_1} \qquad (7)$$

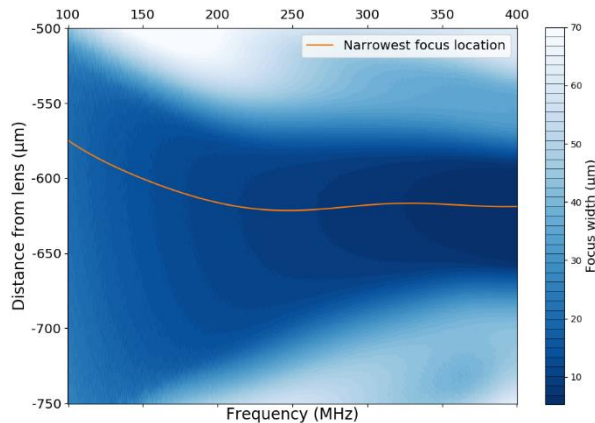where f is frequency, and a_0, a_1, b_1, b_2 and c_1 are fitting parameters.

Figure 7: Frequency dependence of focal width (FWHM) at different distances from the lens. Line shows the point of narrowest focus. Data from frequency domain simulation.

Figure 8 shows the peak intensity and the location of the narrowest focus as a function of frequency in the time- and frequency domain, respectively.
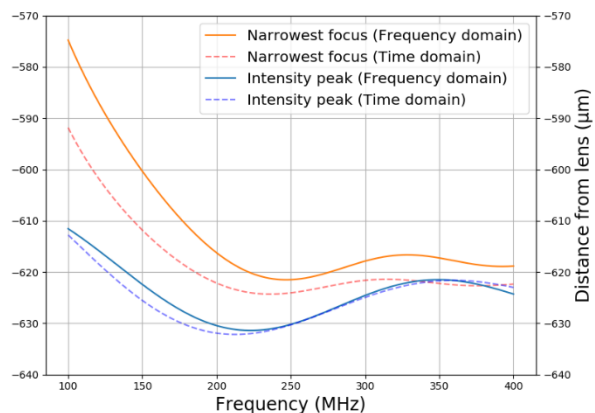

Figure 8: Frequency dependence of the narrowest focus point (orange line) and the point of highest intensity (blue line). Dashed lines show corresponding results obtained in the time domain simulation.

Conclusions

We showed that the SAM lens focuses different frequencies in different ways. The peak intensity is located slightly further away from the lens than the point of narrowest focus (Fig. 8).

Our results make it possible to enhance the imaging resolution of a SAM by providing a model of how to digitally postprocess microscope data. The enhanced image could be constructed either by only taking into account the frequencies that are in focus, or by constructing the image from several images, obtained from different distances.

References

[1] Hesjedal T., Surface acoustic wave-assisted scanning probe microscopy—a summary, Reports on Progress in Physics 73, 2010, p. 1

[2] da Fonseca Raul J.M., Ferdj-Allah L., et al., Scanning Acoustic Microscopy-Recent Applications in Materials Science, Advanced Materials 5, No. 7, 1993, p. 510

[3] Briggs Andrew, Kolosov O.V., Acoustic microscopy 2nd ed, Oxford University Press, 2010, p. 22-23, 48-60, 104-105

[4] Khuri-Yakub B.T., Scanning acoustic microscopy, Ultrasonics, Vol 31 No 5, 1993, p. 362

[5] Gilmore R.S., Industrial ultrasonic imaging and microscopy, J. Phys. D: Appl. Phys. 29, 1996, p. 1395-1396

[6] Meriläinen Antti, Acoustic Microscopy with High Imaging Fidelity, Submitted, 2018

[7] Nolvi A., Kassamakov I., Hæggström E., Subsurface metrology using scanning white light interferometry: absolute z coordinates deep inside displays, J. Opt. Soc. Am. A 35, A18-A22, 2018

[8] Goodwin Eric P., Wyant James C., Field guide to interferometric optical testing, SPIE Press cop, 2006, p. 9

[9] MT-Berlin: http://www.mt-berlin.com/frames_cryst/descriptions/sapphire.htm, Retrieved 23.9.2018.

[10] Advanced Optics: https://www.advancedoptics.com/SodaLimeGlassTechnicalDataSheet.pdf, Retrieved 23.9.2018.

Appendix

Table 1: Material properties used in simulation

Material	Density (kg/m^3)	Young's Modulus (GPa)	Poisson's ratio
Sapphire[9]	3980	345	0.27
Soda-lime glass[10]	2440	72	0.22